JOURNAL OF CATALYSIS 97, 480–492 (1986)

Sorption–Diffusion in Molecular Sieves

II. Aromatics in Y and ZSM-5 Zeolites

LUCIO FORNI[1] AND CARLO F. VISCARDI

Dipartimento di Chimica Fisica ed Elettrochimica, Università di Milano, Via Golgi 19, 20133 Milan, Italy

Received October 23, 1984; revised July 9, 1985

Thermodynamic and kinetic parameters relating to the sorption–diffusion of benzene and methylbenzenes in zeolites Y and ZSM-5 were determined at 613–713 K by the gas chromatographic pulse method. The effects of the various phenomena involved have been separated and the relative energy parameters determined. In NaY zeolite, the thermodynamic parameter was found to grow rapidly with increase in the number of methyl groups carried by the aromatic ring, while the kinetic parameter, relating to the intracrystalline process, decreases. In ZSM-5, no substantial change was noted in the thermodynamic parameter on increasing the number of methyl groups, but the intracrystalline mass-transfer rate was much higher for *p*-xylene than for benzene or toluene. The major resistance to intracrystalline mass transfer in ZSM-5 seems to be connected with the gas–solid interphase-crossing process, sorption–desorption playing a minor role. Partial extraction of lattice Al, with formation of cationic species, was also observed to take place during ion exchange and calcination of zeolite samples.

INTRODUCTION

The so-called decationated (protonated) forms of Y and ZSM-5 zeolites are very active catalysts for a number of reactions of practical interest, among which isomerization, disproportionation, and transalkylation of methylbenzenes and alkylation of aromatics with methanol may be cited (*1–5*). Mass-transfer and sorption–desorption phenomena of methylbenzenes in such catalysts play an important role in determining activity and selectivity, due to the particular structure of these solids.

The present work deals with the determination of thermodynamic and kinetic parameters relating to the sorption–diffusion of benzene and of some methylbenzenes in porous pellets made from zeolitic powder cake, at temperatures (613–713 K) typical for the above-mentioned reactions.

NOMENCLATURE

A	Contribution to peak spreading due to axial eddy diffusion, cm
B	Contribution to peak spreading due to molecular diffusion, $cm^2\ s^{-1}$
C_b, C_i, C_k	Contributions to the van Deemter parameter C, connected with molecular diffusivity, intracrystalline "diffusion," and Knudsen diffusion in macropores, respectively, s
D_{ij}, D_k	Bulk and Knudsen diffusion coefficients, $cm^2\ s^{-1}$
d_c, d_p	Diameters of zeolite crystal and pellet, cm
G_b, G_k	Constants for evaluation of C_b and C_k, respectively
$g_i(P_r)$	Correction factor for pressure drop along the column
HETP	Height equivalent to a theoretical plate, cm
I_s	Severity index during ion exchange
K	Thermodynamic parameter for adsorption process
K_{ads}	Equilibrium constant for sorption–desorption, $cm^3\ g^{-1}$
k_{des}	Rate constant for desorption, s^{-1}

[1] To whom correspondence should be addressed.

0021-9517/86 $3.00

k_{-s} Rate constant for interphase-crossing process, cm s^{-1}
L Bed length, cm
M Adsorbate molecular weight, g mol^{-1}
R_p Radius of pellet, cm
u_s° Superficial rate of carrier gas, cm s^{-1}
W Bed weight, g

Greek Symbols

δ_{int} Kinetic parameter relative to intracrystalline process, s
ε External void fraction of the bed of particles
θ Internal void fraction of pellet
ρ_p Density of pellet, g cm^{-3}
μ_1', μ_2 First absolute and second central moment of the peak
τ Tortuosity factor for diffusion in pellet macropores

METHOD

The gas chromatographic (GC) pulse method adopted is described and discussed extensively in Part I (*6*), together with the apparatus employed. The most interesting parameters for the present study are the thermodynamic constant K_{ads} relating to the sorption–desorption process and the kinetic parameter $1/\delta_{int}$, connected with the time constant relating to the intracrystalline process. These parameters may be determined from the values of the moments μ_1' and μ_2 of the GC peak, the latter being connected with the height equivalent to a theoretical plate (HETP) of the GC column. K_{ads} can be calculated directly from the values of μ_1' and of the geometric parameters of the column, such as the external void fraction ε and length L. The evaluation of $1/\delta_{int}$ may be achieved from the dependence of HETP on carrier gas flow rate u_s°, after separating the contributions due to diffusion in the gas film surrounding the particle and within the macropores of the pellet. The values of two constants, G_b and G_k, connected with bulk and Knudsen diffusion effects, respectively, may then be determined. Such values are obtainable from the dependence of the behavior of the GC column on the nature of the carrier gas and on the dimensions of solid particles, respectively.

EXPERIMENTAL

Adsorbates. Analytical grade chemicals (C. Erba or Merck) were employed as adsorptives (adsorbates). They were carefully dried on precalcined 5A zeolite spheres and then stored over 5A as desiccant, which was frequently renewed.

Carrier gas. Ultrapure helium (SIAD UP, ≧99.9999 mol%) was used as carrier. It was further purified by means of a double-wall glass trap, filled with precalcined (823 K) 13X zeolite, and cooled in liquid nitrogen. A few runs were also performed with high-purity nitrogen (SAPIO PPL, ≧99.999 mol%).

Zeolites. NaY zeolite (SK40) was kindly supplied by Union Carbide as cake, i.e., as binderless, crystalline powder. ZSM-5 was prepared in a single, relatively large (ca. 30 g) batch, in our laboratory, by the hydrothermal method, in a PTFE-lined autoclave. The procedure suggested in the Mobil patent (*7*) was slightly modified, in order to obtain zeolite crystals of larger diameters. X-Ray diffractometric analysis (Debye method) on the "as prepared" powder showed a practically complete crystallization of the zeolite, whose diffractometric pattern was identical to that reported in the literature. A portion of the ZSM-5 cake was subjected to separation by elutriation in distilled water, collecting fractions of different-size crystals. The Al content of the zeolite was determined by chemical analysis, through standard procedure (*8*), and confirmed by atomic absorption spectroscopy. The size of the zeolite crystals was measured on several micrographs obtained by scanning electron microscopy. X-Ray diffractograms of the samples separated by elutriation showed that all such fractions were fully crystalline, except the finest one (average crystal size 1 μm), in which some amorphous material was observed.

Preparation of GC column and procedure. Both the "as supplied" NaY and the "as prepared" NaZSM-5 zeolites showed a marked residual catalytic activity, due to the presence of acidic centers. An ion-exchange treatment was therefore needed, and this was effected by means of saturated NaCl solution, the pH of which was kept at the desired value by adding the proper amount of NaOH. The solid was then washed chloride free (AgCl test) with water to which some drops of NaOH solution were added to keep the pH constant. A final rapid rinsing in distilled water followed. An acidic form of the zeolite was also prepared, by repeatedly treating the powder at 363 K with saturated NH_4Cl solution (*9*). After drying (423 K) and calcination (823 K overnight in dry air) the powder was pressed (maximum pressure 200 MPa) into 1- to 2-mm thick wafers. The wafers were then gently crushed and sieved, collecting the desired mesh fraction, usually 0.18–0.25 mm (60–80 mesh). The latter proved to be a good compromise between excessive pressure drop and the risk of bypass of the carrier gas through the column. After packing, the column was pretreated *in situ* at 773 K for 12 h in a slow flow of dry air, followed by the carrier gas (793 K, 24 h). Temperature was then lowered to the desired value and the injection of adsorbate pulses started. The principal characteristics of the GC columns employed are summarized in Table 1.

The procedure followed for data collection and processing is given in detail in Part I (*6*). To summarize, after checking the validity of the assumptions upon which the method relies, the steps were as follows:

(i) Evaluation of the geometric parameters (ε, L, W, etc.) of the column.

(ii) Evaluation of the moments μ_1' and μ_2 of the peak.

(iii) Evaluation of the van Deemter parameters B and C_b and of the thermody-

TABLE 1

Characteristics of the GC Columns Employed

Column No.	Zeolite	pH during ion exchange	Average particle diam, d_p (cm)	Average zeolite crystal diam, d_c (μm)	Column length, L (cm)	Bed weight, W (g)	External void fraction, ε	Al content as Al_2O_3 (wt%)
L1	NaY	7	0.020	1	22.6	0.800	0.46	23.5
L30	NaY	11–12	0.040	1	22.6	0.899	0.23	
L31	NaY	11–12	0.017	1	14.0	0.495	0.31	
L32	NaY	11–12	0.020	1	16.0	0.586	0.34	
L28	HY	5.5	0.020	1	17.1	0.703		
L33	NaZSM-5	11–12	0.020	7.5	14.6	0.618	0.31	2.19
L14	NaZSM-5	11–12	0.020	7.5	12.0	0.472	0.37	
L15	NaZSM-5	12–13	0.020	4	15.0	0.550	0.36	3.17
L17	HNaZSM-5	[a]	0.020	4	9.55	0.379	0.37	5.04
L21	NaZSM-5	7	0.020	4	9.70	0.407	0.39	
L24	NaZSM-5	11–12	0.020	4	8.60	0.386	0.34	2.20
L19	NaZSM-5	11–12	0.020	2.5	15.0	0.606	0.39	3.11
L16	HZSM-5	5.5	0.020	2.5	12.3	0.561		
L25	NaZSM-5	[b]	0.020	2.5	10.3	0.443	0.36	2.65
L26	NaZSM-5	11–12	0.020	1	8.50	0.330	0.32	3.25
L18	HZSM-5	[c]	0.020	~5	13.2	0.620		

[a] From the "as prepared" cake, elutriated, but not subjected to ion exchange.
[b] From L16 zeolite, by back exchange (pH 11–12).
[c] From the "as prepared" cake, by ion exchange with NH_4Cl (pH 5.5).

namic parameter K relating to sorption–desorption equilibrium. The latter parameter is related to the equilibrium constant K_{ads} by the equation $K_{ads} = K/\rho_p$, ρ_p being the density of the zeolite pellet.

(iv) Calculation of the curve, fitting the HETP vs u_s° data (Fig. 1), and evaluation of van Deemter parameters A and C_{i+k}.

(v) Evaluation of the contribution to C_{i+k} of parameter C_k, connected with Knudsen diffusion in macropores.

(vi) Evaluation of kinetic parameter $1/\delta_{int}$ (s^{-1}), relative to the intracrystalline process.

(vii) Calculation of the van't Hoff and Arrhenius parameters relating to K_{ads} and to $1/\delta_{int}$, respectively.

RESULTS AND DISCUSSION

Contribution of Bulk Diffusivity to Mass-Transfer Resistance

This contribution has been evaluated by determining the effect of changing the carrier gas on the value of the van Deemter parameter C_b for a given column under identical experimental conditions, employing the equation (*6*)

$$\left(\frac{\text{HETP}}{g_2} - \frac{\varepsilon B}{u_s^\circ}\right)_{N_2} - \left(\frac{\text{HETP}}{g_2} - \frac{\varepsilon B}{u_s^\circ}\right)_{He} = (A_{N_2} - A_{He}) + \frac{1}{\varepsilon}(C_b)_{He}\left(\frac{D_{a,N_2}}{D_{a,He}} - 1\right) u_s^\circ \quad (1)$$

in which the diffusion coefficients D_{a,N_2} and $D_{a,He}$ were calculated by the standard procedure (*10*).

Runs were performed on column L30 (see Table 1) with benzene as adsorbate and He or N_2 as carrier gas. From the parameters of the straight lines (least-squares) obtained by plotting the first member of Eq. (1) vs u_s°, the following values of $C_{b,He}$ were calculated: 1.13×10^{-4}, 0.99×10^{-4}, and 0.85×10^{-4} s at 633, 653, and 673 K, respectively. From these values and by means of the equation

$$C_b = \frac{d_p^2}{30(1-\varepsilon)} \frac{G_b}{D_{AB}} \quad (2)$$

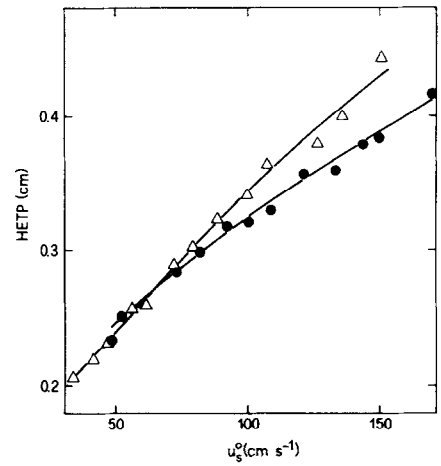

FIG. 1. Typical fitting of the calculated HETP vs u_s° curve with respect to experimental points. Column, L19; adsorbate, benzene. (△) 673, (●) 633 K.

the average value $G_b = 8.08 \pm 0.72$ was calculated for the mentioned temperature range. As a first approximation, this value was employed for both Y and ZSM-5 zeolites. In fact, the particles packing the columns were prepared by the same procedure, i.e., by pressing the zeolite cake under identical conditions.

Zeolite Y

Separation of the effect of Knudsen diffusion and of the intracrystalline mass-transfer process. The separation is made possible by the different influence of particle size on the two processes. The equation employed is

$$C_{i+k} = C_i + 3.44 \times 10^{-6} G_k \frac{\varepsilon d_p^2}{1-\varepsilon} \sqrt{M/T} \quad (3)$$

where

$$C_i = \frac{2\varepsilon}{1-\varepsilon} \frac{\delta_{int}}{K}. \quad (4)$$

Experimental data were collected on columns L30, L31, and L32, of particle sizes 0.017, 0.020, and 0.04 cm, on the average, respectively. From Eq. (3) one obtains

$$y = G_k + \frac{\delta_{int}}{K} x \quad (5)$$

where

$$y = \frac{(1 - \varepsilon)C_{i+k}\sqrt{T/M}}{3.44 \times 10^{-6}\varepsilon d_p^2}$$

$$x = \frac{2\sqrt{T/M}}{3.44 \times 10^{-6} d_p^2}$$

so that, by plotting y vs x, a straight line (least-squares) was obtained at each temperature (Fig. 2), the slope of which gave the following values of (δ_{int}/K): 3.94×10^{-4}, 3.13×10^{-4}, and 3.02×10^{-4} s at 633, 653 and 673 K, respectively. The intercepts of the three straight lines practically converge to the same value, as expected, so that an average value of $(8.32 \pm 0.25) \times 10^5$ cm^{-1} was calculated for the constant $G_k = \tau/\theta R_p$. It may be noted that, by assuming $\tau/\theta \cong 4$, as usually suggested (*10*) for similar systems, one obtains $R_p = 4.8 \times 10^{-2}$ μm. This is a reasonable value for the average size of macropores in particles obtained by pressing, at relatively low pressure, crystals with diameters of the order of ca. 1 μm.

Influence of methyl groups present on the aromatic ring. Experimental problems grow rapidly with increase in the number of methyl groups carried by the aromatic ring. The simultaneous increasing of sorbate reactivity and of retention time quickly reduces the range of experimental conditions within which the effect of chemical reactivity on the second moment μ_2 is negligible, as requested by the assumptions on which the present method relies. As a consequence, sound data could be collected only for benzene, toluene, and *o*-xylene. Kinetic data for *m*- and *p*-xylene could be obtained at only two temperatures, differing by 25 K, due to a progressive slow fouling of the zeolite. As for mesitylene, only thermodynamic data were found to be reliable. The results are shown as van't Hoff or Arrhenius plots in Fig. 3. In Table 2 (upper part) the values for enthalpy and entropy changes connected with the sorption process are reported, together with the values for the apparent activation energy and the

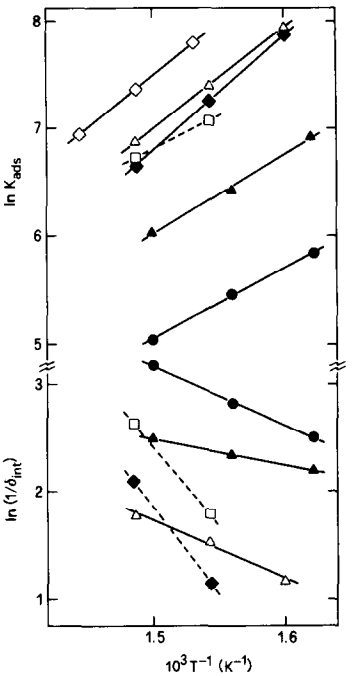

FIG. 3. Van't Hoff and Arrhenius plots, for equilibrium constant relative to sorption of methylbenzenes, and for kinetic parameter relative to intracrystalline process, respectively, in NaY zeolite. Column, L1. (●) Benzene, (▲) toluene, (□) *p*-xylene, (◆) *m*-xylene, (△) *o*-xylene, (◇) mesitylene.

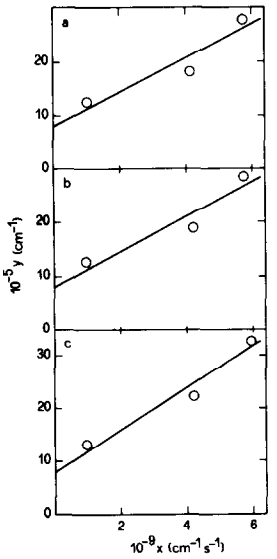

FIG. 2. Plot of y vs x (Eq. (5)). Adsorbate, benzene; columns, L30, L31, and L32. (a) 633, (b) 653, (c) 673 K.

TABLE 2

Enthalpy and Entropy of Sorption and Apparent Activation Energy and Arrhenius Preexponential Factor of Intracrystalline Process

Adsorbate	$-\Delta H_{ads}$ (kcal mol^{-1})	$-\Delta S_{ads}$ (e.u.)	E_a (kcal mol^{-1})	ln A
		NaY zeolite		
Benzene	13.1 ± 0.1	9.5 ± 0.2	10.9 ± 0.2	11.5 ± 0.2
Toluene	15.0 ± 0.6	10.4 ± 1.0	5.1 ± 0.7	6.4 ± 0.6
o-Xylene	18.2 ± 0.01	13.3 ± 0.02	10.3 ± 1.3	9.5 ± 1.0
m-Xylene	19.3 ± 0.4	14.9 ± 0.7	(34.3)[a]	(27.9)
p-Xylene	(14.9)	(8.7)	(30.5)	(25.6)
Mesitylene	18.8 ± 0.2	13.2 ± 0.3	—	—
		NaZSM-5 zeolite		
Benzene	22.1 ± 0.3	21.8 ± 0.5	21.5 ± 2.5	16.6 ± 1.9
Toluene	22.4 ± 0.6	22.0 ± 0.9	19.7 ± 1.1	15.1 ± 0.8
p-Xylene	24.2 ± 0.05	25.1 ± 0.08	15.9 ± 2.5	13.1 ± 1.9

[a] In parentheses are those data collected at only two temperatures (648 and 673 K), due to slow, progressive fouling of the zeolite.

Arrhenius preexponential factor relating to the intracrystalline process. These values have been calculated from the parameters of the straight lines (least-squares) fitting the experimental data in Fig. 3. The following observations may be made:

(i) The value of the thermodynamic constant K_{ads} grows rapidly on increasing the number of methyl groups present on the aromatic ring. Such an increase is connected mainly with the rapid increase of the enthalpic term, while the entropic one does not change remarkably (Table 2).

(ii) Although no reliable kinetic results could be obtained for mesitylene and only incomplete data for *m*- and *p*-xylene, the rate of the intracrystalline mass-transfer process, as expressed by the parameter $1/\delta_{int}$, appears to decrease on increasing the number of methyl groups. In any case, the mass-transfer process seems to be much faster for *p*-xylene than for *o*- or *m*-xylene.

(iii) The kinetic parameter changes more slowly than the thermodynamic one. As a consequence, the overall resistance to mass transfer, expressed as δ_{int}/K, decreases on increasing the number of methyl groups.

Zeolite ZSM-5

Influence of zeolite crystal size. Experiments have been performed on columns L26, L19, L24, and L33, made from samples obtained by elutriating the same batch of ZSM-5 zeolite. The entire set of columns was prepared under exactly identical conditions. The columns differed only by the size of the zeolite crystals in the pellets (see Table 1). Only benzene was used as sorbate. As reported in detail in Part I (*6*), the dependence of δ_{int} on the diameter d_c of the zeolite crystals is expressed by three different equations, namely,

$$\delta_{int} = \frac{d_c^2}{60D_i} \tag{6}$$

if the rate-determining step (rds) of the intracrystalline process is Fickian diffusion within the micropores,

$$\delta_{int} = \frac{d_c}{6k_{-s}} \tag{7}$$

if the resistance is localized at the external surface of the crystal, and

$$\delta_{int} = 1/k_{des} \tag{8}$$

if the rds is sorption–desorption on the micropore walls. In Eqs. (6)–(8), D_i is the effective diffusion coefficient of adsorbate in the zeolite micropores, k_{-s} is the rate constant, referred to the unit external surface area of the crystal, for the interphase-crossing process of sorbate leaving the crystal, and k_{des} is the rate constant, referred to unit volume of the crystal, for the sorbate desorption process. As regards the thermodynamic parameter K_{ads}, no dependence on d_c is expected. The experimental data have been treated by taking $G_b = 8.08$ and $G_k = 8.32 \times 10^5$ cm^{-1}, i.e., the values previously obtained for NaY zeolite. Experimental results are given in Fig. 4. One may observe that the K_{ads} values are practically independent of d_c, except for the finest crystals (L26 column, average crystal diameter $d_c = 1$ μm). This was probably connected with the above-mentioned presence of amorphous material, as revealed by X-ray diffractograms, since the value of K_{ads} depends on the mass of zeolite packed in the

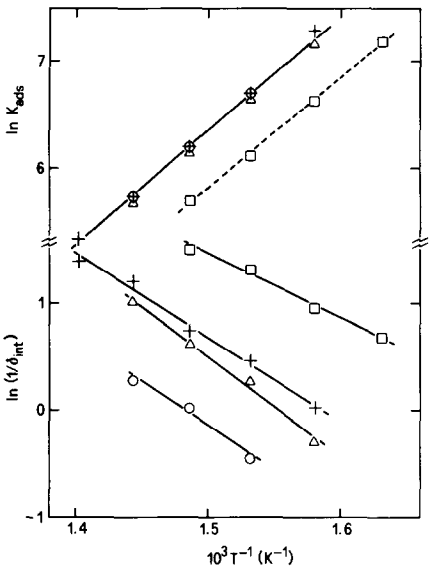

FIG. 4. Dependence of K_{ads} and of $(1/\delta_{int})$ on zeolite crystal diameter for benzene on NaZSM-5. d_c (μm) = 1 (□), 2.5 (+), 4 (△), 7.5 (○).

column. A similar dependence is not expected for the values of $1/\delta_{int}$. In any case, the parameters of the best straight lines (least-squares), drawn through the experimental points of Fig. 4, permitted the values of $-\Delta H_{ads} = 20.6 \pm 0.4$, 22.0 ± 0.5, 21.6 ± 0.1, and 21.8 ± 0.4 kcal mol^{-1} and $-\Delta S_{ads} = 19.3 \pm 0.6$, 20.3 ± 0.7, 19.8 ± 0.1, and 20.0 ± 0.6 e.u. to be calculated for d_c = 1, 2.5, 4, and 7.5 μm, respectively. This confirms that, in all cases, adsorption centers of the same type are involved for all the fractions, with average $-\Delta H_{ads} \cong 21.5$ kcal mol^{-1} and $-\Delta S_{ads} \cong 19.9$ e.u.

As regards the $1/\delta_{int}$ data, unfortunately experimental points could not be collected over the whole range of temperature (613–713 K) for every column, due to the abovementioned limits for useful experimental conditions. As a consequence, a more complete representation (Fig. 5) of the dependence of δ_{int} on d_c could be obtained only after calculating two lacking points (reported in parentheses in the figure) by means of the Arrhenius parameters evaluated from the plots of Fig. 4. One may note that the Fig. 5 data lie satisfactorily along straight lines at every temperature. This permits us to eliminate Fickian diffusion (Eq. (6)) as the rds of the intracrystalline mass-transfer process. Furthermore, the best straight lines (least-squares), drawn through the data of Fig. 5, present a positive intercept value, so that, in principle, neither mechanism (Eqs. (7) and (8)) representing the rds should be discarded. However, as the value of the intercept is relatively small, the major resistance to mass transfer is very probably connected with the interphase-crossing process (Eq. (7)), the sorption–desorption effect (Eq. (8)) playing a minor role. The intercept, i.e., the value of δ_{int} at $d_c = 0$, represents the contribution to mass-transfer resistance, connected only with the sorption–desorption process from the zeolite surface. As a consequence, the value of k_{des} was evaluated from such intercept values and by Eq. (8), obtaining the data shown as an Arrhenius plot in Fig. 6 (upper line). From this plot, an apparent activation energy for the adsorption–desorption process $E_a = 7.5 \pm 0.8$ kcal mol^{-1} was calculated, together with $\ln A = 8.1 \pm 0.6$ for the corresponding preexponential factor.

On the other hand, the slope of the straight lines of Fig. 5 was used, together with Eq. (7), for evaluating the rate constant k_{-s} of the interphase-crossing pro-

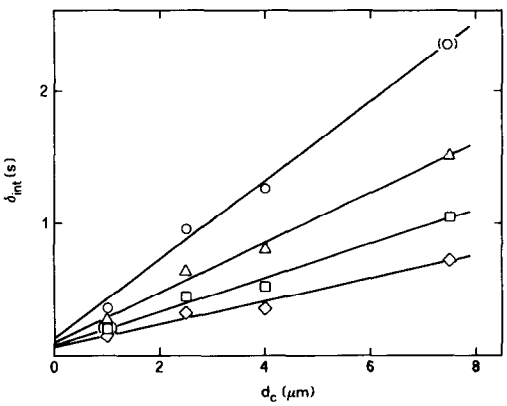

FIG. 5. Evaluation of k_{des} and k_{-s} (see text) for benzene on NaZSM-5. (○) 633, (△) 653, (□) 673, (◇) 693 K.

cess. The Arrhenius plot shown in the same Fig. 6 (lower line) was thereby obtained, from which the values of $E_a = 18.3 \pm 0.1$ kcal mol^{-1} and $\ln A = 13.4 \pm 0.1$ were calculated for the energy parameters connected with the process. The present data then indicate that the intracrystalline process probably involves two subsequent steps: desorption from the micropore walls and the overcoming of a barrier localized at the crystal–gas interphase, i.e., at the pore mouth. By taking into account all our data, a semiquantitative picture of the overall process can be represented as shown in Fig. 7 (solid lines). In such a scheme, both steps require an activation energy lower than the enthalpy gap between the initial and final states. This is in agreement with many published data (*11–13*) reporting activation energy values for the mass-transfer process lower than the enthalpy of adsorption. In other words, the ratio δ_{int}/K_{ads}, i.e., the energy parameter connected with the resistance to the intracrystalline process, is always found to increase with increasing temperature.

However, these results cannot be considered as definitive, since our zeolite fractions, although coming from the same batch of cake, did not show the same chemical composition. As reported in Table 1, the Al content rises from 2.19 to 3.25 (wt%, expressed as Al_2O_3) with decreasing crystal diameter. This is probably connected with the method of preparation of our zeolite. When ZSM-5 is formed by crystallization

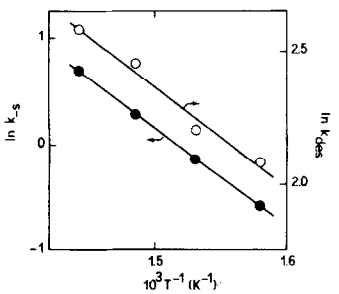

FIG. 6. Arrhenius plot for k_{des} (○) and k_{-s} (●). System: benzene–NaZSM-5.

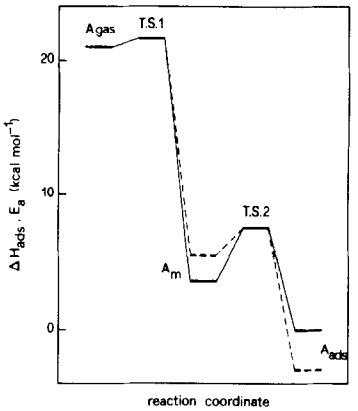

FIG. 7. Scheme of the energy changes involved in the intracrystalline process for benzene (solid lines) or *p*-xylene (dashed lines) in NaZSM-5. T.S. = transition state intermediate; A_{gas}, A_m, A_{ads} = sorbate A, in gas phase, in micropores, adsorbed on pore walls.

under hydrothermal conditions, with silica gel as the source of silica as in the present case, a progressive decrease of the Al content is observed from the core to the external shell of the crystal. This effect has been attributed (*14*) to the progressive decrease of the Al^{3+} concentration in the mother gel, with formation of an Al-deficient outer shell of ZSM-5 or of isostructural silicalite. Additional causes of radial gradients in the Al concentration could be connected with the procedure followed during ion exchange and/or calcination. In Table 1 one may observe that the Al content of all the elutriated fractions is lower than that measured for the precursor cake. In the present case, dealumination seems not to be connected with processes taking place during ion exchange. In fact, when considering columns L15 and L24, prepared from the same fraction of elutriated zeolite, one can see that the Al concentration is higher in L15, which was subjected to ion exchange under more severe conditions. The phenomenon seems to be better explained by assuming that, during calcination to eliminate the alkylammonium or ammonium ions, a part of the Al migrates out of the zeolite lattice, with formation of cationic dihydroxyaluminum species, which are sub-

sequently leached out during ion exchange. Such an interpretation, also proposed by others (*3, 15*) in similar cases, is confirmed by a comparison between the behavior of the L19 and L25 columns: both come from the same fraction of elutriated ZSM-5 and both were Na-exchanged and subsequently calcined under identical conditions. However, L25, which presents a lower concentration of Al, was subjected to NH_4^+ exchange and calcination before the final Na^+ exchange. The process is summarized in some detail in Fig. 8. Finally, it cannot be excluded that a linear increase of δ_{int} with d_c^2, as expected for a Fickian diffusion process, could have been masked by the progressive decrease of the Al content. This would lead to a corresponding decrease in the number of relatively cumbersome Na^+ ions, thereby increasing the width of the zeolite channels.

Decationated zeolite. Owing to the very effective catalytic properties of the acidic form of both Y and ZSM-5 zeolites, benzene is the only aromatic useful as adsorbate, in that it is the least reactive one. However, with both zeolites in the acidic form (columns L28, L16, and L18) the adsorption isotherms were found to be nonlinear, even at the lowest concentration of adsorptive (adsorbate) in the carrier gas detectable by our flame ionization detector, at any column temperature (523–723 K). In any case, from a qualitative point of view, a much lower retention time was observed, for both zeolites, with respect to their Na form. This corresponds to a lower value of adsorption equilibrium constant, as if adsorption centers were "weaker" in the acidic than in the sodium form.

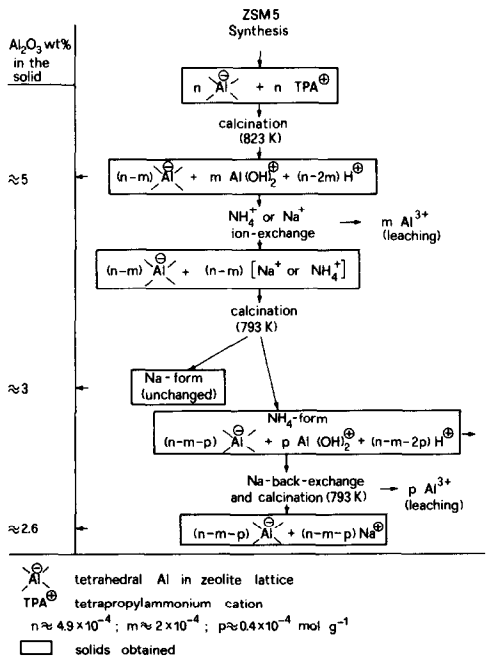

FIG. 8. Possible mechanism for the dealumination observed in ZSM-5 samples.

Effect of ion-exchange conditions for NaZSM-5. Two series of comparative runs were conducted, benzene being the adsorbate for both series. The entire set of columns employed was prepared from the same fraction of elutriated zeolite, but the pH of the Na-exchanging solution was progressively increased up to 12–13, going from L17 to L21, L24, and L15 columns, in that order (see Table 1). A severity index I_s = pH − pNa = $\log(C_{Na^+}/C_{H^+})$ was introduced, referred to the ion-exchanging solution. Results are shown in Fig. 9.

Acidic centers being "weaker" than sodium ones, the value of equilibrium constant should grow with an increase in the severity of the ion-exchange treatment. Such behavior is verified only for I_s from 2 to 7, K_{ads} values decreasing by further increases in I_s up to 11 and 13. The phenomenon could be due to nonfacile access to the adsorption centers, because of the increasing blocking of zeolite pores by Na^+ ions. This hypothesis is supported by the value of the enthalpy change $-\Delta H_{ads} = 21.8 \pm 0.3$ kcal mol^{-1}, which is found to be independent of severity, indicating that adsorption sites of the same type are involved in all samples.

On the other hand, the kinetic parameter $1/\delta_{int}$ is practically independent of severity, for I_s = 2–7, but decreases on further increasing I_s. This behavior as well is easily explained by the progressive reduction of

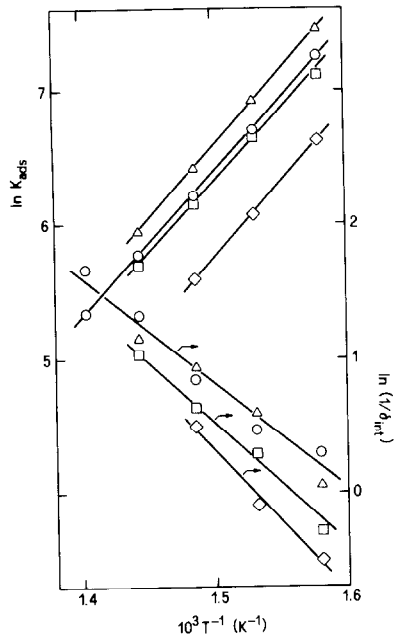

FIG. 9. Effect of severity of ion-exchange treatment. System, benzene–NaZSM-5. I_s = (○) 2, (△) 7, (□) 11, (◇) 13.

pore width with increasing number of Na^+ ions in zeolite channels. The apparent activation energy and the corresponding Arrhenius preexponential factor, connected with the $1/\delta_{int}$ parameter relating to the gas–solid process, were calculated by considering together the data relating to I_s = 2 and 7. The results are E_a = 15.3 ± 2.5, 18.8 ± 1.2, and 21.5 ± 2.4 kcal mol^{-1} and ln A = 12.6 ± 1.1, 14.8 ± 0.9, and 16.6 ± 1.9, for I_s = 2–7, 11, and 13, respectively.

Effect of ion back exchange in NaZSM-5. This study was carried out by means of columns L25 and L19 (Table 1), prepared from the same fraction of elutriated zeolite. The ion-exchange steps were the following. A part of the decationated zeolite employed for column L16 was Na-back-exchanged at pH = 11–12 to obtain the zeolite for column L25. Column L19 was prepared from the zeolite "as obtained" from elutriation, by Na-exchanging at the same pH. Experimental runs were made with benzene as adsorbate and results are shown in Fig. 10. The severity index being the same for both columns, the marked difference in both the thermodynamic and kinetic parameters depends only on some irreversible change taking place on decationated sites during the preparation of the protonated form. The Na-back-exchange procedure restores only in part the original adsorption capacity of the zeolite, the value of K_{ads} for the L19 column being ca. 1.6 times higher than that for L25 column at any temperature.

On the other hand, both enthalpy and entropy changes ($-\Delta H_{ads}$ = 21.7 ± 0.5 and 22.0 ± 0.5 kcal mol^{-1} and $-\Delta S_{ads}$ = 20.8 ± 0.7 and 20.3 ± 0.7 e.u., respectively) are practically the same for the two columns. The difference in the values of the thermodynamic constant seems then to be connected with a decrease in the number of adsorption sites rather than with a decrease of their strength. This confirms that a part of the original sites is lost during preparation of the decationated form, as previously reported (Fig. 8). In the present case, for the zeolite of column L25, a decrease of Al content by ca. 15% has been measured (Table 1), with respect to the L19 sample, accompanied by a decrease of the K_{ads} value of ca. 35%. It may be concluded that the HZSM-5 obtained through NH_4^+ exchange, followed by calcination at 793 K, has been dehydroxylated by ca. 20%. In such a zeolite, ca. 15% Al is present in cationic form

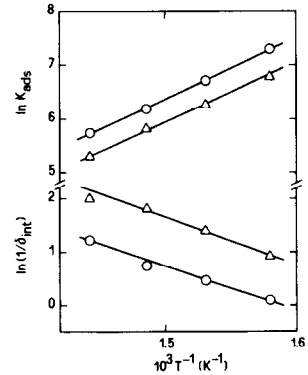

FIG. 10. Effect of Na back exchange. Sorbate, benzene. (○) NaZSM-5, (△) back-exchanged NaZSM-5. I_s = 11 in final Na exhange for both samples.

and occupies ca. 15% of the adsorption sites.

As regards the kinetic parameters, the data of Fig. 10 show that in back-exchanged zeolite the mass-transfer process is much more rapid. This is very likely to be due to increased opening of the zeolite pores because of the lower number of Al atoms in the lattice, leading to a smaller number of Na^+ ions. The apparent activation energy of the process remains practically unchanged (16.0 ± 1.9 and 15.9 ± 1.0 kcal mol^{-1}, with ln A = 13.7 ± 1.5 and 12.7 ± 0.8, respectively, for the L25 and L19 columns), indicating that the mechanism of the process is probably the same for both zeolites. The present data then confirm that both ion-exchange and calcination conditions can strongly modify the structure of zeolitic material, thereby affecting considerably the sorption–diffusion (and catalytic) properties of these solids.

Effect of activation temperature. Columns L14 and L33 were prepared from the same fraction of elutriated and Na-exchanged ZSM-5 (Table 1), the only difference being the temperature (713 and 793 K, respectively) of the activation performed *in situ* just before starting adsorbate (benzene) injections. The behavior of such columns shows that the increasing of the pretreatment temperature leads to an increase in K_{ads} (by ca. 40%) and to a decrease in $1/\delta_{int}$ (by ca. 10%) at any temperature. However, only a small decrease (from 23.7 ± 0.2 to 21.8 ± 0.4 kcal mol^{-1} and from 23.5 ± 0.3 to 20.0 ± 0.6 e.u.) was noted in $-\Delta H_{ads}$ and in $-\Delta S_{ads}$, respectively, the apparent activation energy remaining practically unchanged (17.6 ± 0.4 and 17.1 ± 3.3 kcal mol^{-1}, with ln A = 13.3 ± 0.3 and 12.8 ± 2.5, respectively).

Effect of methyl groups present on the aromatic ring. Experiments concerning this effect could be made only on the L15 column, i.e., on the zeolite exchanged under the most severe conditions (I_s = 13). All other columns showed a more or less marked catalytic activity of the methylated benzenes, thus preventing the collection of reliable data. It was also immediately observed that only the behavior of toluene and *p*-xylene could be analyzed in some detail. *o*- and *m*-xylene and polymethylbenzenes showed a very short retention time, close to that of nonadsorbed substances. The experimental results, shown in Fig. 11 and Table 2 (lower part), are very different from those obtained with NaY zeolite (Fig. 3). The strong increase in K_{ads} on increasing the number of methyl groups does not appear any longer. Equilibrium constants for toluene are only slightly higher and those for *p*-xylene are even lower than those for benzene. $-\Delta H_{ads}$ values rise very slowly with increase in the number of methyl groups, but the effect on the values of K_{ads} is balanced or more than balanced by the corresponding increase in $-\Delta S_{ads}$. This may be connected with the progressive decrease in mobility of adsorbate molecules within the zeolite pores. As regards the kinetic parameters, it may be observed that the rate of the intracrystalline process decreases slightly from benzene to toluene, but grows considerably from tolu-

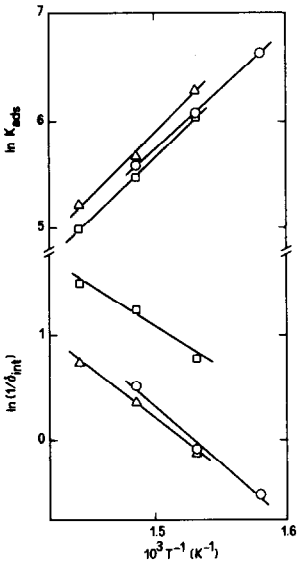

FIG. 11. Effect of methyl groups present on the aromatic ring in NaZSM-5. (○) Benzene, (△) toluene, (□) *p*-xylene.

ene to *p*-xylene, whose values of $1/\delta_{int}$ are practically twice as high as those for benzene. The apparent activation energy (Table 2) decreases regularly from benzene to *p*-xylene. This quite surprising behavior (*16*) has been confirmed in our laboratory on many different ZSM-5 samples, coming from a variety of preparations and employing different precursor gels, leading to ZSM-5 samples with SiO_2/Al_2O_3 ratios ranging from ca. 15 up to ca. 31.

Recalling the two-step mechanism previously mentioned for the intracrystalline process, the present results indicate that, on going from benzene to *p*-xylene, energy levels would shift as shown by the dashed lines in Fig. 7. It may be seen that on increasing the number of methyl groups, the energy difference $A_m - A_{ads}$ between the intermediate within the micropore (A_m) and the adsorbed substance (A_{ads}), increases more rapidly than the overall energy change ΔH_{ads} connected with the progressive change in adsorption energy.

CONCLUSIONS

The results of the present work may be summarized as follows.

(i) In both NaY and NaZSM-5 zeolites the resistance connected with the intracrystalline process provides the major contribution to the overall sorption–diffusion process, at least for low-diameter (0.02–0.04 cm) granules.

(ii) The values of the thermodynamic and kinetic parameters and the chemical analysis data relating to zeolite samples treated in different ways show that there is a marked effect on the characteristics of the zeolite from the conditions at which both ion exchange and calcination are performed.

(iii) Acidic ZSM-5 zeolite shows a much lower adsorption equilibrium constant and much more rapid sorption–diffusion kinetics, with respect to the sodium form.

(iv) Calcination is accompanied by some irreversible structural transformation, even at temperatures usually considered well below those at which the zeolite crystal lattice becomes unstable. Such a transformation involves mainly the decationated (protonated) sites and leads to a decrease in reticular Al content. This also suggests that the calcination treatment, usually performed to decompose the residual alkylammonium ions, trapped in the "as prepared" ZSM-5 cake, should be properly controlled.

(v) The most probable rds of the intracrystalline process in ZSM-5 is the interphase gas–crystal barrier crossing, sorption–desorption from pore walls playing a minor, but not negligible, role. However, some further study is needed to separate better the effects of chemical inhomogeneity, present even in fractions of different crystal size, coming from the same batch of ZSM-5 cake.

In spite of the quite strong limitations involved (*6*), the GC pulse method employed in the present study has proved to be a simple, rapid, and reliable way to collect interesting and useful information on the sorption–diffusion of relatively bulky molecules in zeolite granules, particularly for the comparison of the behavior of different samples within a given range of experimental conditions.

ACKNOWLEDGMENT

The valuable help of Dr. D. Sudati in collecting some of the experimental data is gratefully acknowledged.

REFERENCES

1. Weisz, P. B., *Chemtech.* **3,** 498 (1973).
2. Weisz, P. B., *Pure Appl. Chem.* **52,** 2091 (1980).
3. Breck, D. W., "Zeolite Molecular Sieves." Wiley, New York, 1974.
4. Csicsery, S. M., *in* "Zeolite Chemistry and Catalysis" (J. A. Rabo, Ed.), ACS Monogr. 171, p. 680. Amer. Chem. Soc., Washington, D.C., 1976.
5. Dwyer, J., *Chem. Ind.*, p. 258 (1984).
6. Forni, L., Viscardi, C. F., and Oliva, C., *J. Catal.* **97,** 469 (1986).
7. Argauer, R. J., and Landolt, G. R., U.S. Patent 3,702,886, Nov. 1972.
8. Treadwell, F. P., "Chimica Analitica," Vol. II. Vallardi, Milan, 1962.

9. Bolton, A. P., *in* "Experimental Methods in Catalytic Research" (R. B. Anderson and P. T. Dawson, Eds.), Vol. II, p. 17. Academic Press, New York, 1976.
10. Satterfield, C. N., "Mass Transfer in Heterogeneous Catalysis." MIT Press, Cambridge, Mass., 1970.
11. Ma, Y. H., and Mancel, C., *Adv. Chem. Ser.* **121,** 392 (1973).
12. Bülow, M., Struve, P., Finger, G., Redszus, Ch., Ehrhardt, K., and Schirmer, W., *J. Chem. Soc. Faraday Trans. 1* **76,** 597 (1980).
13. Ruthven, D. M., *Amer. Chem. Soc. Symp. Ser.* **40,** 320 (1977).
14. Derouane, E. G., Detremmerie, S., Gabelica, Z., and Blom, N., *Appl. Catal.* **1,** 201 (1981).
15. Bolton, A. P., and Lanewala, M. A., *J. Catal.* **18,** 154 (1970).
16. Wu, P., Debebe, A., and Ma, Y. H., *Zeolites* **3,** 118 (1983).